HYBRID PROPULSION FOR A MOON SAMPLE RETURN MISSION

C. Schmierer[(1),(3)], M. Kobald[(1)], J. Steelant[(2)], and S. Schlechtriem[(1)]

[(1)] DLR, Institute of Space Propulsion, Langer Grund, 74239 Hardthausen, Germany
christian.schmierer@dlr.de, konstantin.tomilin@dlr.de, mario.kobald@dlr.de, stefan.schlechtriem@dlr.de

[(2)] ESA-ESTEC, TEC-MPA, Propulsion Design and Aerothermodynamics Section
Keplerlaan 1, 2200 AG Noordwijk, The Netherlands
johan.steelant@esa.int

[(3)] Institute of Space Systems, University of Stuttgart, Pfaffenwaldring 29, 70569 Stuttgart, Germany
schmierer@irs.uni-stuttgart.de

KEYWORDS

Hybrid rocket propulsion, moon sample return, propulsion system analysis, trajectory analysis

ABSTRACT

A hybrid propulsion mission to the Moon with the goal of sample return is designed and analysed based on the knowledge gained with hybrid propulsion at the University of Stuttgart and the DLR Lampoldshausen. Advantages and disadvantages are compared and the feasibility of an European Technology Demonstrator Mission is checked. A trajectory analysis of a launcher is done in order to estimate the possible payload in Moon transfer orbit. This payload is the reference mass for the analysed spacecrafts. Six different variants of hybrid propulsion spacecraft are designed and compared, as well as two liquid propulsion spacecraft. The performance is compared and the payload in form of sample return mass is determined. Hybrid propulsion with new advanced fuels that take advantage of liquefying melt layers can provide higher thrust to weight ratios than classical fuels and therefore enable missions with hybrid propulsion that until recently seemed unfeasible. The payload of a high performance hybrid propulsion spacecraft is comparable to liquid propellant systems and at the same time uses green propellants and offers a low-cost approach by reducing development and operation costs.

1 INTRODUCTION

A sample return mission to the Moon is both of interest for scientists and for technology demonstration of hybrid propulsion. Hybrid propulsion is known since long, however in the shadow of liquid and solid propulsion in the last decades not much effort was put into hybrid propulsion to mature the technology. Only in the recent 20 years worldwide research and technology projects started to improve hybrid propulsion technology. Many applications are analysed in the last years including orbital propulsion [1], space debris removal [2], planetary missions [3] and sounding rockets of student teams [4, 5] and companies [6]. Hybrids potentially offer fail-safe space transportation comparable to air transport [7]. Even new futuristic concepts like air-breathing hybrid rocket engines are researched [8]. One incentive for the hybrid propulsion technology advancement was the improvement on liquefying fuels made by Karabeyoglu et al [9]. Those fuels have a higher regression rate and allow the development of high thrust to weight ratios in the hybrid engines. The paraffin-based liquefying fuels have since then been steadily improved in regression rate behaviour and mechanical properties [10]. In this study it is investigated, how a sample return mission, which lands on the Moon's surface, gathers samples and scientific data and launches them back to Earth, could be realized with the use of hybrid propulsion. Hybrid propulsion has many advantages like storability of "green" propellants, safety in development and operations, cheap propellants, and yet high performance even in the environments in space. New paraffin-based fuels have increased the regression rate and therefore decreased the complexity of hybrid rocket engines even further. A sample return mission is simulated and optimized using state of the art software ASTOS and EcosimPro/ESPSS in order to validate the feasibility of hybrid propulsion in a mission to Moon. Different mission concepts are compared using different launch vehicles, different spacecraft set-ups and different propellants. Hybrid propulsion technology can decrease cost and development time in the future of space exploration and in the same time offer non-toxic, green propellants. At the DLR Lampoldshausen and the University of Stuttgart the technology in the field

of hybrid propulsion with paraffin-based fuels has continuously been advanced in the last years and the newest insights are used for this analysis, because only highly developed hybrid propulsion can compete with the high technology level of liquid propulsion systems. Examples of the recent advancements are the development of a new paraffin-based fuel with improved regression rate and mechanical behaviour [11, 12, 13] at the DLR Lampoldshausen and the launch of the record breaking student sounding rocket HEROS at the University of Stuttgart [4, 14, 15]. This work is based on previously published work on the Hybrid Moon Lander [16].

2 SOFTWARE

In order to analyse, simulate and optimize vehicles with hybrid rocket engines a tool for ASTOS® 8 (Analysis, Simulation and Trajectory Optimization Software for Space Applications) has been developed. This tool uses analytical equations to simulate the hybrid rocket combustion process and give predictions about the performance over time. The tool also includes a connection loop to Ecosim-Pro/ESPSS (European Space Propulsion System Simulation). This connection is used to simulate the propulsion system with an ESPSS model of the same and compare the results of analytical tool prediction and the ESPSS model. Information about how the hybrid tool for ASTOS works and some proof work can be found in [17].

3 MISSION TRAJECTORY

Several launchers are potentially able to launch a spacecraft to Moon. In order to reduce the amount of necessary optimizations only one launch vehicle was used to form a baseline for the sample return mission: Ariane 5. For the mission analysis a direct launch into a Moon transfer trajectory was chosen as a reference, which means that the Ariane 5 is launching the spacecraft with its upper stage into a transfer orbit to the Moon. The spacecraft is not conducting impulse maneuvers in LEO. Trajectory optimization showed, that the total mass of the spacecraft launched by an Ariane 5 in that trajectory is about $8800\,\mathrm{kg}$. It is basically following the elliptical transfer orbit of a Hohmann transfer. The flight time until the Moon flyby is about five days. Figure 1 shows the trajectory of the spacecraft from Earth's surface to a Moon flyby in 100 km altitude. This capture point of the Moon is at the same time close to the apogee in the Earth-centered reference frame. The excess velocity at the flyby is about $860\,\mathrm{m\,s^{-1}}$. The inclination at the Moon is $90°$. In this orbital plane every spot on the lunar surface can be reached with phasing orbits (with long-time storable propellants). For the lander spacecraft the mission design considers a course correction during the approach to the Moon. At the perilun the first impulsive maneuver with about $850\,\mathrm{m\,s^{-1}}$ ΔV is conducted to enter a elliptical orbit around Moon with a perilun of about $30\,\mathrm{km}$. After half a revolution when the spacecraft reaches the new perilun, the engines are fired again in two consecutive burns in order to produce another ΔV of about $1740\,\mathrm{m\,s^{-1}}$. In between those two burns the spacecraft descends further closer to the surface and reaches $1\,\mathrm{km}$ after that. By now only the final lander stage is remaining. A hovering phase of one minute is included to allow finding a suitable landing spot, which needs another $100\,\mathrm{m\,s^{-1}}$. After another coast the final soft landing is taking place which needs about $100\,\mathrm{m\,s^{-1}}$ again. In total the ΔV for landing is about $2790\,\mathrm{m\,s^{-1}}$ to $2810\,\mathrm{m\,s^{-1}}$ depending on the spacecraft set-up. Figure 2 shows the altitude over time of the landing and Figure 3 depicts the details of the final $4\,\mathrm{km}$. The color shows the different phases. The trajectory is the one of a three staged hybrid propulsion lander. The phase durations are a bit different for other concepts however the overall trajectory stays quite similar. In the detailed view the hovering phase is visible as well as the soft landing phase.

Figure 4 shows the velocities and speed during the landing trajectory. The flight path speed is shown together with the velocity in the three directions. The relative east velocity component takes the rotation of the celestial body into account and therefore is the surface fixed east velocity. The ΔV can also be compared in that diagram, seeing that the first deorbit burn at $100\,\mathrm{km}$ altitude is small compared to the final descent maneuver and landing. The relative east velocity and the north velocity have a huge change between $2000\,\mathrm{s}$ and $2500\,\mathrm{s}$. This is due to the fact, that the spacecraft passes by the lunar south pole and the reference system changes

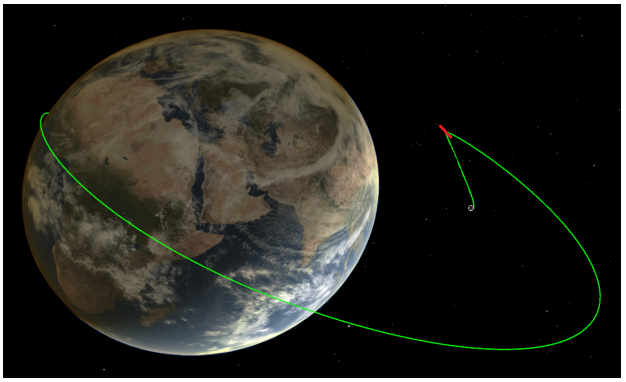

Figure 1: Moon transfer trajectory of a Ariane 5 launched spacecraft

quickly. The speed basically stays the same. In Figure 5 the hovering phase and the final landing is shown in detail. It can be seen that the spacecraft is still descending a little bit during the hovering. This is due to the fact, that the constraints for the optimization were not that strict in order to make the optimization with ASTOS find an optimal result faster. After the hovering the radial velocity is increasing again in a short coast phase. Then it continues to increase but slower, when the engines are ignited but throttled down. After 3625 s the engines are throttled up an the lander decelerates for a soft touch down. The north and radial velocity during the last descent are always zero.

The optimization with ASTOS optimizes the spacecraft's set-up as well as the phase durations and the controls. The attitude and throttle control are shown in the Figures 6, 7 and 8. A smooth control is usually a sign for a optimal solution in ASTOS. If there are extreme spikes and jumps the result is suggesting that it is not optimal yet, but needs further refinement. The depicted curves are considered well optimized. The x-axis is not showing time but the independent variable, in which every phase is exactly of the length 1, regardless how long the phase actually is. This allows the optimizer to keep phases with extremely long and short duration in a good weight to each other in the optimization process.

3.1 ASTOS Model Setup

A short description of how the trajectory model was set up in ASTOS is given in the following paragraph. The optimization process is steered by the user by adjusting the phases, initial and final boundary constraints for each phase, as well as path constraints along the phases, if necessary. The landing trajectory starting at the perilun of the hyperbolic fly-by is separated in nine phases: 1. Orbit Capture Burn; 2. Coast Arc #1; 3. De-Orbit & Deceleration Burn #1; 4. Coast Arc #2; 5.

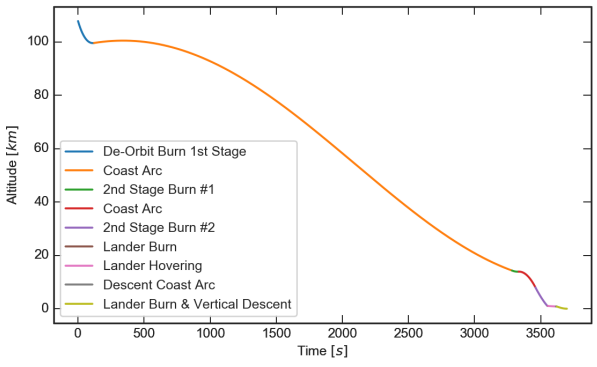

Figure 2: Altitude over time of the Moon lander

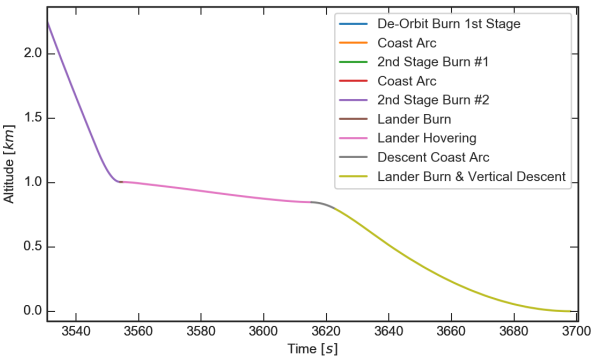

Figure 3: Altitude over time of the Moon lander (detail)

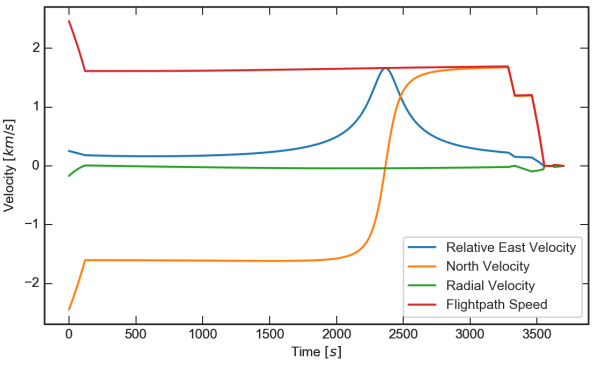

Figure 4: Velocity over time of the Moon lander

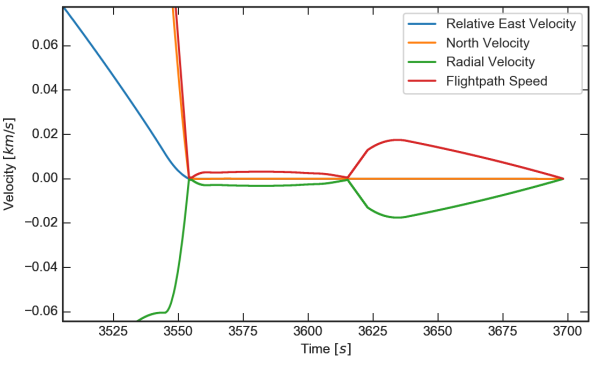

Figure 5: Velocity over time of the Moon lander (detail)

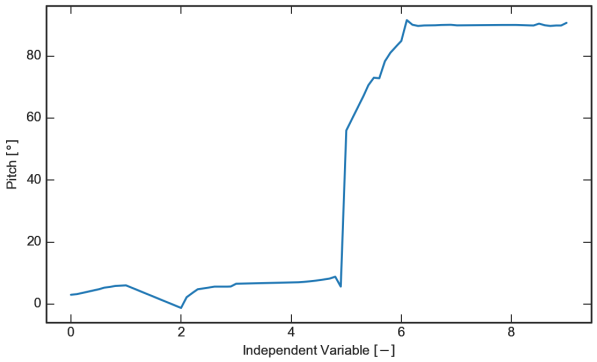

Figure 6: Pitch over independent phase variable

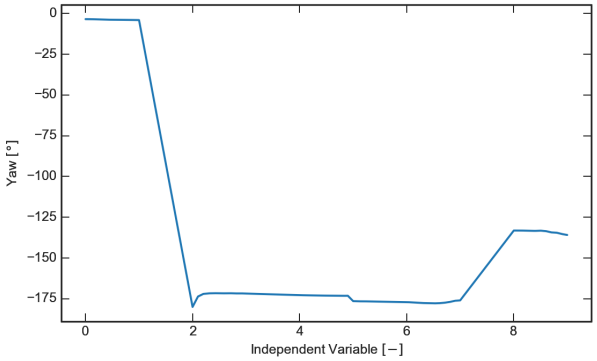

Figure 7: Yaw over independent phase variable

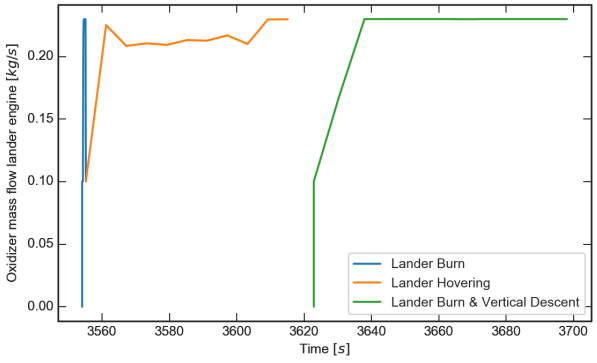

Figure 8: Oxidizer mass flow of a single lander engine

Deceleration Burn #2; 6. Lander Burn; 7. Lander Hovering; 8. Descent Coast; 9. Vertical Descent and Landing. In the two staged variants the first stage is doing the burns in all phases prior to phase 6 where the lander is separated. For the three staged variants the first "orbit capture" burn is done by the first stage which is then jettisoned. The constraints are listed in the following:

- Mass Initial Boundary Constraint: After substracting $300\,\mathrm{kg}$ propellant for course correction from the total launcher payload of $8800\,\mathrm{kg}$, $8500\,\mathrm{kg}$ remain. For cryogenic propellants the boil-off needs to be considered as well.
- Altitude Final Boundary Constraints:
  - Phase 1: $100\,\mathrm{km}$
  - Phase 6 & 7: $0.85\,\mathrm{km}$ to $1\,\mathrm{km}$
  - Phase 9: $0\,\mathrm{m}$ to $1\,\mathrm{m}$
- Altitude Path Constraints:
  - Phase 7 - $0.85\,\mathrm{km}$ to $1\,\mathrm{km}$
- Apolun Final Boundary Constraint:
  - Phase 1 - $100\,\mathrm{km}$
- Perilun Final Boundary Constraint:
  - Phase 1 - $10\,\mathrm{km}$ to $30\,\mathrm{km}$
- Radial Velocity Final Boundary Constraint:
  - Phase 6 & 7: $-0.5\,\mathrm{m\,s^{-1}}$ to $0.5\,\mathrm{m\,s^{-1}}$
- Radial Velocity Path Constraint:
  - Phase 7: $-5\,\mathrm{m\,s^{-1}}$ to $0\,\mathrm{m\,s^{-1}}$
- North Velocity Path Constraint:
  - Phase 9: $-0.1\,\mathrm{m\,s^{-1}}$ to $0.1\,\mathrm{m\,s^{-1}}$
- Relative East Velocity Path Constraint:
  - Phase 9: $-0.1\,\mathrm{m\,s^{-1}}$ to $0.1\,\mathrm{m\,s^{-1}}$
- Flightpath Speed Path Constraint:
  - Phase 9: $0\,\mathrm{m\,s^{-1}}$ to $0.5\,\mathrm{m\,s^{-1}}$

In order to improve the optimization speed and results a lot of tweaking to the model needed to be done. Next to the constraints, controls, the grid and optimizer set-up as well as the initial guess are very important. The initial guess is the initial trajectory set by the user, which needs already to be very close to the final orbit. A combination of trial and error as well as doing preliminary optimizations of certain phases with less parameters is used to find a suitable initial guess. The optimization was also done in steps: The constraints were activated in several steps because it is impossible to optimize

constraints which are violated by a large margin. One example is the final altitude at the landing, which should be zero according to the constraint. The initial guess however will cause the altitude at the end of the last phase to be e.g. $40\,\mathrm{km}$ below the surface. The optimization has difficulties to find the correct solution if the initial guess is so far off. Therefore first all the other phases and constraints are optimized in steps to slowly reach the final correct and also optimal trajectory. The optimization is set to collocation method with 29 major grid nodes in the long coast phase. For a reference about the optimization methods see [18] and the ASTOS user manual. All other phases are initialized with only 1 major grid node and optimized with Runge Kutta 4/5 multiple shooting method. After some testing this set-up has proven to be the fastest optimization for the trajectory of this mission. The control (pitch, yaw and oxidizer mass flow) was refined with 9 nodes in every phase.

4 PROPULSION SYSTEM

4.1 Hybrid Propulsion Basics

A hybrid rocket motor uses a liquid oxidizer and a solid fuel. Classical solid fuels are polymers and HTBP, which cause problems as they have an extremely slow regression rate. The regression rate in a hybrid rocket motor is not pressure dependent but is limited by the heat transfer to the fuel's surface and is simplified described as a function of oxidizer mass flux density.

$$\dot{r} = aG_{ox}^{n} \tag{1}$$

The fuel mass flow is then determined by the fuel surface and the oxidizer mass flux density. With a low regression rate, the fuel surface needs to be very large. And as very long fuel grains are impractical, the only way to design hybrid rocket engines with classical fuels is to cast them in complex shapes which offer a larger surface area. Most common are the waggonwheel design, star shapes or multiport designs. Those designs often have a drawback as they are more complex to cast and also have fuel remainings because if the fuel is regressing to the end some larger fuel junks might break off and damage the engine. Therefore with waggonwheel and multiport fuel grains the engine has to be shut off before the fuel is depleted completely. At the DLR Lampoldshausen paraffin-based fuels have been advanced for this reason. Paraffin has a low melting point and therefore forms a liquid layer in the hybrid rocket combustion chamber. The liquid film forms waves which on the one hand increase the surface and on the other enforce the entrainment of droplets into the gas flow, which increases the regression rate as the heat transfer to the surface is not such a limiting factor anymore. The paraffin-based fuels have been optimized for their regression rate behaviour and mechanical properties by adding additives [11, 13]. At the DLR Lampoldshausen and the University of Stuttgart, nitrous oxide and gaseous oxygen were used. Recently the test bench capability has been augmented with liquid oxygen. Another very promising oxidizer is H_2O_2 which can be stored for a long time, used as a mono propellant as well, which is useful both for engine ignition and spacecraft attitude control systems. One major problem of hybrid propellants currently is the efficiency. The combustion process happens along the fuel grain's surface and as the flame is within the boundary layer flow of the fuel grain, mixing of fuel and oxidizer can be problematic. For that reason often modifications to the post-combustion chamber are necessary, which is increasing the structural mass. Therefore for the simulations and optimizations in this paper a comparably low combustion efficiency of $90\,\%$ has been used.

4.2 Propellant Comparison

The mission design was also compared with storable and cryogenic liquid propellant systems. Table 1 lists the specific impulse in vacuum condition, the assumed engine efficiency and the mixture ratio for the compared engine systems with an expansion ratio of 100. Dinitrogen tetroxide and hydrazine represent the storable liquid propellant combination, LOX & methane the cryogenic propellant combination. Both liquid propellant combinations have a higher estimated efficiency, as it is standard technology to have high efficiencies. PB-5% is a paraffin-based fuel with $5\,\%$ additives (in mass).

4.3 Propulsion System Simulation

For one spacecraft layout the propulsion system simulation in the ASTOS hybrid tool has been compared to the ESPSS model simulation results. The schematic of the ESPSS model is shown in Figure 9. The model includes a pressurization tank with $300\,\mathrm{bar}$ Helium, a valve, a pressure regulator, an oxidizer tank and the necessary piping connecting

Table 1: Propellant comparison for the Moon mission

Parameter	$\overline{I_{vac}}$	η_{eng}	O/F
NTO & hydrazine	$3300\,\mathrm{m\,s^{-1}}$	$95\,\%$	1.4
LOX & LCH_4	$3553\,\mathrm{m\,s^{-1}}$	$95\,\%$	3.4
H_2O_2 & PB-5%	$2950\,\mathrm{m\,s^{-1}}$	$90\,\%$	7.5 to 7.6
LOX & PB-5%	$3280\,\mathrm{m\,s^{-1}}$	$90\,\%$	2.8 to 2.9

Note: Expansion ratio $\epsilon = 100$

the tank to the engine. The stages have four parallel engines while the model has only one engine. A oxidizer outflow which mirrored three times the oxidizer flow through the first engine was used to mimic the same oxidizer usage as in all four engines. The Figure 10 shows the mass flow for the respective simulations. The oxidizer tank is pressurized to 30 bar at the beginning of the simulation via the pressure regulator from the Helium reservoir. The injector pressure drop aims at 10 bar resulting in a chamber pressure of about 18 bar with additional pressure losses in pipes and valves. The oxidizer mass flow can be controlled by a proportional-integral-derivative (PID) controller, in order to have the same oxidizer mass flow as in the ASTOS simulation, where the oxidizer mass flow is an active control as well. A rocket stage with two burning phases and H_2O_2 as the oxidizer was compared. The first burn starts at 10 s and ends roughly 45 s later. The second burn starts at 100 s and takes roughly 95 s. It is easily visible that there is no difference in the static parts of the simulation. The only difference in the mass flow starts during the last 15 s of the second burn: this is when the pressurization in the ESPSS model reaches a too low pressure and the tank pressure cannot be kept up. The oxidizer tank pressure decreases and with it the mass flow of the oxidizer. The thrust is shown in Figure 11. The diagram shows no difference except for the afore mentioned decrease at the end of the ESPSS simulation. Another minor expected difference is the gradient behaviour at the beginning of each burn phase. The regression rate is modelled equally in both models with the regression rate law $\dot{r} = aG_{ox}^{n}$, hence it was expected to find no big discrepancy between the models.

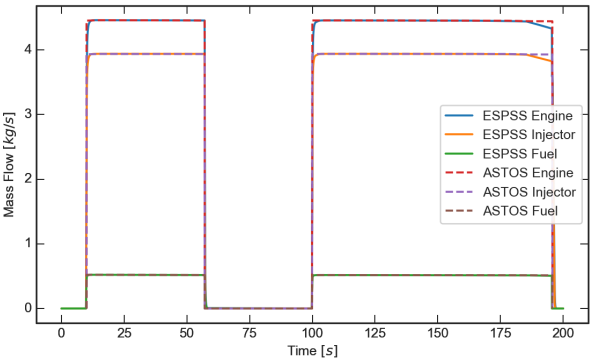

Figure 10: Mass flow simulation comparison

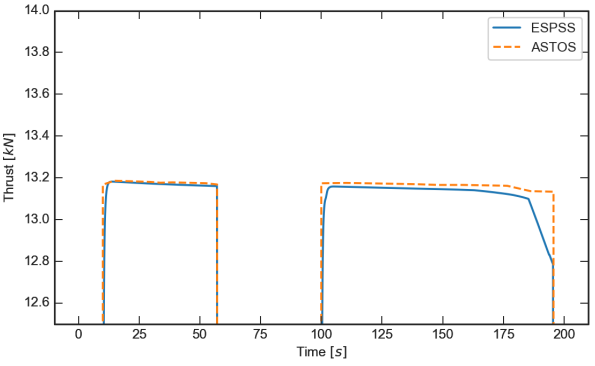

Figure 11: Thrust simulation comparison

5 MASS ESTIMATION

All masses of the spacecraft and its subsystems need to be estimated in order to evaluate the payload capacity of the sample return mission. Most estimations were done by a quick literature survey and simple estimations. This holds especially true for all instrumentation etc. For several subsystems

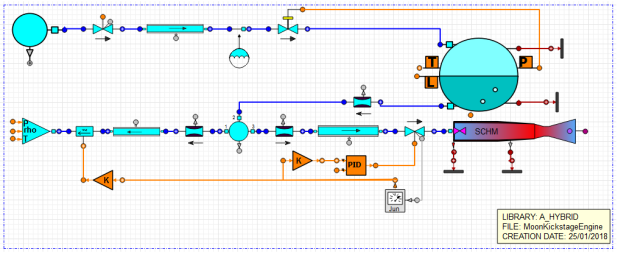

Figure 9: Simulation schematic in ESPSS

the mass estimations for the lander stage are listed in Table 2. For all stage structures the same assumptions have been taken: the structural mass is always $7.5\,\%$ and the staging adapter adds another $1.5\,\%$ of the total stage mass. The liquid propellant tanks are calculated as a spherical pressure vessel with $25\,\mathrm{bar}$ working pressure and a safety factor of 2 using composite mateirals. Additionally $15\,\mathrm{kg}$ of feed lines and valves are considered, as well as the helium mass and pressurization tank mass. The hybrid rocket engines are estimated with CFRP combustion chamber walls scaled with pressure loads and mass estimations for chamber insulation, nozzle extension and aluminium and brass injector parts.

6 SPACECRAFT VARIANTS

In order to compare the propulsion system choices three staging variants have been chosen:

- Variant 1: a three staged lander concept (similar to the ones described already in [16]). Two expendable boost/kick stages are providing the necessary ΔV to the landing stage. The kick stages have four rocket engines each with a thrust of about $13\,\mathrm{kN}$.
- Variant 2: a two staged lander concept. Only one expendable boost/kick stage is foreseen. This kick stage has 8 engines with $13\,\mathrm{kN}$ each, firing them in groups of four simultaneously.
- Variant 3: a two staged lander concept, but this time the boost/kick stage jettisons some structural mass of the first 4 depleted hybrid engines half way through the total burning time.

All variants use a single staged return rocket, which is launched from atop of the lander stage. For all three variants in the hybrid propulsion version the three resp. two stages are using either H_2O_2 and PB-5% or LOX and PB-5%. The return rocket always uses H_2O_2 as an oxidizer as long term storage is necessary. All cryogenic fluids are cooled with boil-off, which is calculated as a fixed percentage per day to evaporate during the flight to the Moon. The liquid propellant systems were simulated with the two staged variant only. As ane example the Variant 1,2 and 3 with H_2O_2 as an oxidizer are compared in their masses in Table 3. It is easily visible that the three-staged system is more optimal for the higher return rocket mass which corresponds to a higher payload (soil sample) mass. However, the two-staged variant might be more suitable for from a mission cost-perspective because less components need to be developed. The return rocket mass needs to be compared to the bi-liquid variants in order to evaluate the performance of the hybrid propellant spacecrafts. Table 4 lists the return rocket mass and the corresponding soil sample mass for all simulated variants. The soil sample was calculated with a flyback trajectory to Earth, the resulting necessary ΔV and the mass estimations for the return rocket's subsystems. The return rocket mass and sample mass naturally are linked. Therefore with a higher return rocket mass the sample return mass is going to be larger as well. It is visible that the variants 1 to 3 of the hybrid propulsion spacecraft are in a similar range and the bi-liquid spacecrafts have a higher sample return mass. Between the hybrid propulsion spacecraft the 3 staged version has the highest sample return mass and using LOX improves the sample mass also, even if then boil-off oxidizer has to be considered. The gain in specific impulse outweighs the losses due to boil-off. It is also notable that the two staged concept with jettisoning of empty engines (variant 3) is nearly as effective as the variant 1. Of course jettisoning engines might be more difficult but it allows to save some parts on the oxidizer supply line. The question is, why the hybrid propulsion systems are performing lower than the liquid systems. The answer is not one simple reason. It is the combination of many. First of all, the tank shape for liquid propellants allow to reduce the structural mass per tank volume to an optimum. The cylindric shape of a hybrid rocket chamber that stores the solid fuel is not optimal. The engines can get long and/or thick and have a higher structural mass ratio. Saving on insulation material might help here in future developments. The next reason is of course the engine efficiency which plays a major role. However the current technology level of hybrid rocket engines does not allow the same efficiency in hybrid like in liquid systems without increasing the structural mass by prolonging post combustion chambers and mixing devices. However, the last line in the table shows variant 1 with LOX with $95\,\%$

Table 2: Mass estimations for spacecraft design

Subsystem	Mass estimation
Power supply	35 kg
Flight computer unit	8 kg
Thermal control	100 kg
Telemetry & communication	35 kg
GNC	11 kg
Others	25 kg
Driller	70 kg
Manipulator arm	70 kg
Scientific instruments	150 kg
Landing Legs	130 kg
Rover	100 kg

Table 3: Mass comparison for H_2O_2 and PB-5%

	Variant 1	Variant 2	Variant 3
Total spacecraft	8800 kg	8800 kg	8800 kg
First kickstage	2986 kg		
H_2O_2	2233 kg		
PB-5%	247 kg		
Propellant reserve	20 kg		
Structure engines	90 kg		
Structure oxidizer	64 kg		
Structural mass	332 kg		
Second kickstage	3154 kg	6292 kg	6237 kg
H_2O_2	2349 kg	4728 kg	4667 kg
PB-5%	296 kg	561 kg	559 kg
Propellant reserve	20 kg	40 kg	40 kg
Structure engines	90 kg	181 kg	181 kg
Structure oxidizer	65 kg	132 kg	131 kg
Structural mass	334 kg	650 kg	659 kg
Lander stage	1337 kg	1341 kg	1356 kg
H_2O_2	318 kg	332 kg	339 kg
PB-5%	23 kg	25 kg	26 kg
Propellant reserve	2 kg	2 kg	2 kg
Structure engines	19 kg	22 kg	22 kg
Structure oxidizer	9 kg	9 kg	9 kg
Structural mass	966 kg	951 kg	958 kg
Return rocket	1323 kg	1167 kg	1207 kg

combustion efficiency and this reduces the gap to the bi-liquid engines by a huge margin. The last reason for the higher performance of the liquid engines is, that the burning time of a combustion chamber is not limited by the capability to store fuel inside the chamber. The liquid engine maximum burn duration in a single or in consecutive burns is limited only by material fatigue. A hybrid combustion chamber is limited in size as a large diameter to store more fuel is bad for both the structural mass as well as the flow conditions because if the flow area gets to big the oxidizer mass flux density will decrease to very small numbers. The hybrid propulsion system has some disadvantages regarding structural mass of the system, maximum burn duration and combustion efficiency. The efficiency can be solved in future with advantage of the technology level. Then the difference compared to bi-liquid systems gets smaller. If the performance loss is small, it can be other considerations that can make the hybrid propulsion spacecraft more attractive for the application in a spacecraft in comparison to bi-liquid systems:

- Lower cost of development: It is suggested, that the development cost of a hybrid propulsion system can be smaller as it has less components compared to a bi-liquid system.
- Lower cost of operation: Only the oxidizer needs to be handled at the launch site. Most launch vehicles are already based on LOX and therefore LOX infrastructure will be already available.
- No explosion hazard: Even if explosions during rocket launches have gotten rarer, it still happens from time to time. The fuel of a hybrid combustion chamber is solid and has a limited surface. It cannot feed an explosion.

If for a space mission only storable propellants are considered for long time mission and dinitrogen tetroxide and hydrazine are not used anymore due to the REACH regulation, the situation has to be evaluated again: if LOX, N_2O_4 and N_2H_4 are not available the specific impulse of a H_2O_2 and PB-5% based hybrid rocket engine is comparable to that of most other storable liquid propellants. A well working replacement of N_2H_4 still needs to be found and the hybrid propulsion systems using H_2O_2 and paraffin based fuel could be very useful to fill that empty spot. Hydrogen peroxide can be ignited with a catalyst bed which allows to have a very simple, reliable ignition system, which allows for reignition of the engine for several times. The storability of hydrogen peroxide is quite well, the decomposition is slow. For deep space missions it is also possible to still use N_2O_4 and mixtures of nitrogen monoxide (MON) as an oxidizer. A study of a mars sample return rocket using MON-30 and paraffin based fuel is done at NASA. Both propellants are well suited for the extreme temperature range on the surface of Mars [3].

7 CONCLUSION

The feasibility of a sample return mission with hybrid propulsion from a system analysis point of view has been proven. Several concepts have been compared using different propellant and staging options. The

Table 4: Mass comparison for return rocket and soil sample

	Propellants	Return Rocket	Soil Sample
Variant 1	H_2O_2 & PB-5%	1323 kg	45 kg
	LOX & PB-5%	1440 kg	54 kg
Variant 2	H_2O_2 & PB-5%	1167 kg	34 kg
	LOX & PB-5%	1355 kg	48 kg
Variant 3	H_2O_2 & PB-5%	1207 kg	37 kg
	LOX & PB-5%	1416 kg	52 kg
Bi-liquid	N_2O_4 & N_2H_4	1545 kg	84 kg
	LOX & Methane	1566 kg	87 kg
Var. 1 95%	LOX & PB-5%	1590 kg	75 kg

analysis showed that the developed tools for ASTOS and ESPSS are working as expected. The performance comparison of hybrid rocket propulsion and liquid propulsion system showed, that hybrid propulsion performance needs still to be increased in order to be comparable to liquid engines. For hybrids with paraffin-based fuels both LOX and H_2O_2 are promising. The first proves higher performance even despite boil-off, the latter provides long-term storability and the ability of reignition with a catalyst. The three staged lander concept yielded the highest performance but is also the most complex one in development and production. The bi-liquid spacecrafts had a higher performance, however the development cost might be higher. In the future hydrazine will be replaced by other propellants and a hybrid rocket engine using H_2O_2 and a paraffin-based fuel might be a adequate choice. Especially for longterm missions where cryogenic propellants cannot be utilized it offers a good solution. The performance of hybrid rocket engines needs to be further improved in order to increase combustion efficiency and decrease the structural mass.

References

[1] Karine Odic et al. “HYPROGEO Hybrid Propulsion: Project Objectives & Coordination”. In: *Space Propulsion Rome*. 2016.

[2] M. Faenza et al. “Hybrid Propulsion Solutions for Space Debris Remediation Applications”. In: *Industrial Days ESA ESTEC*. 2016.

[3] A. Chandler Karp et al. “A Hybrid Mars Ascent Vehicle Concept for Low Temperature Storage and Operation”. In: *52nd AIAA/SAE/ASEE Joint Propulsion Conference*. 2016.

[4] M. Kobald et al. “Hybrid Experimental Rocket Stuttgart: A Low-Cost Technology Demonstrator”. In: *Journal of Spacecraft and Rockets* 55.2 (2018), pp. 484–500.

[5] T. Knop, J. Wink, and et al. “Failure Mode Investigation of a Sorbitol-based Hybrid Rocket Flight Motor for the Stratos II Sounding Rocket”. In: *51st AIAA Joint Propulsion Conference*. 2015.

[6] O. Verberne et al. “Development of the North Star Sounding Rocket: Getting ready for the first demonstration Launch”. In: *51st AIAA Joint Propulsion Conference*. 2015.

[7] A. Takahashi and T. Shimada. “Essentially Non-explosive Propulsion Paving a Way for Fail-Safe Space Transportation”. In: *31st ISTS Japan*. 2017.

[8] Yen-Sen Chen, J. Lin, and S. Wei. “Development of an Airbreathing Hybrid Rocket Booster”. In: *31st ISTS Japan*. 2017.

[9] M. A. Karabeyoglu, D. Altman, and B. J. Cantwell. “Combustion of liquefying hybrid propellants: Part 1, general theory”. In: *Journal of Propulsion and Power* 18.3 (2002), pp. 610–620.

[10] Y. Tang, S. Chen, and L. T. DeLuca. “Mechanical Modifications of Paraffin-based Fuels and the Effects on Combustion Performance”. In: *Propellants, Explosives, Pyrotechnics* (2017).

[11] Mario Kobald et al. “Viscosity and Regression Rate of Liquefying Hybrid Rocket Fuels”. In: *Journal of Propulsion and Power* 33.5 (2017), pp. 1245–1251.

[12] M. Kobald, I. Verri, and S. Schlechtriem. “Theoretical and Experimental Analysis of Liquid Layer Instabilities in Hybrid Rocket Engines”. In: *CEAS Space Journal* 7.1 (Mar. 2015), pp. 11–22.

[13] M. Kobald et al. “Evaluation of Paraffin-based Fuels for Hybrid Rocket Engines”. In: *50th AIAA/ASME/SAE/ASEE Joint Propulsion Conference*. 2014.

[14] Mario Kobald et al. “A Record Flight of the Hybrid Sounding Rocket HEROS 3”. In: *31st ISTS Japan*. 2017.

[15] M. Kobald et al. “Sounding Rocket "HEROS" - A Low-Cost Hybrid Rocket Technology Demonstrator”. In: *53rd AIAA/ASME/SAE/ASEE Joint Propulsion Conference*. 2017.

[16] C. Schmierer et al. “Analysis and Preliminary Design of a Hybrid Propulsion Lunar Lander”. In: *Space Propulsion Conference*. 2016.

[17] Christian Schmierer et al. “Combined Trajectory Simulation and Optimization for Hybrid Rockets using ASTOS and ESPSS”. In: *31st ISTS Japan*. 2017.

[18] P. Gath. “CAMTOS - A Software Suite Combining Direct and Indirect Trajectory Optimization Methods”. PhD thesis. University of Stuttgart, 2002.